pH regulation in an acidophilic green alga – a quantitative analysis

Birgit Bethmann[1] and Gerald Schönknecht[1,2,3]

[1]Julius-von-Sachs-Institut für Biowissenschaften der Universität Würzburg, Lehrstuhl für Botanik I, Julius-von-Sachs-Platz 2, 97082 Würzburg, Germany; [2]Institute for Plant Biochemistry, Heinrich-Heine-University, Universitätsstr. 1, 40225 Düsseldorf, Germany; [3]Oklahoma State University, Department of Botany, Stillwater, OK 74078, USA

Author for correspondence:
Gerald Schönknecht
Tel: +1 405 744 5549
Email: gerald.schoenknecht@okstate.edu

Received: *6 February 2009*
Accepted: *15 March 2009*

New Phytologist (2009) **183**: 327–339
doi: 10.1111/j.1469-8137.2009.02862.x

Key words: adaptation to acidic environment, buffer capacity, green alga, pH regulation, proton transport.

Summary

- Short-term cytosolic pH regulation has three components: H^+ binding by buffering groups; H^+ transport out of the cytosol; and H^+ transport into the vacuole. To understand the large differences plants show in their tolerance to acidic environments, these three components were quantified in the acidophilic unicellular green alga *Eremosphaera viridis*.
- Intracellular pH was recorded using ion-selective microelectrodes, whereas constant doses of weak acid were applied over different time intervals. A mathematical model was developed that describes the recorded cytosolic pH changes. Recordings of cytosolic K^+ and Na^+ activities, and application of anion channel inhibitors, revealed which ion fluxes electrically compensate H^+ transport.
- The cytosolic buffer capacity was $\beta = 30$ mM. Acidification resulted in a substantial and constant H^+ efflux that was probably driven by the plasmalemma H^+-ATPase, and a proportional pH regulation caused by H^+ pumped into the vacuole. Under severe cytosolic acidification (≥ 1 pH) more than 50% of the ATP synthesized was used for H^+ pumping. While H^+ influx into the vacuole was compensated by cation release, H^+ efflux out of the cell was compensated by anion efflux.
- The data presented here give a complete and quantitative picture of the ion fluxes during acid loading in an acidophilic green plant cell.

Introduction

All living cells maintain a cytosolic pH close to neutrality. Proton-coupled transport processes and H^+-consuming or H^+-generating metabolic reactions continuously threaten to change the cytosolic pH, which has to be kept constant within narrow limits. In plant cells, sudden illumination or darkening causes significant cytosolic pH changes that are compensated within a few minutes (Guern *et al.*, 1991; Bethmann *et al.*, 1998). There is increasing evidence that changes in cytosolic pH are a functional part of intracellular signal transduction (Felle, 2001).

Artificial cytosolic pH changes caused by the application of weak lipophilic acids (Fig. 1) have been used for decades to investigate the mechanism and potential of short-term cytosolic pH regulation (McLaughlin & Dilger, 1980; Frachisse *et al.*, 1988). The principal components of this short-term 'biophysical' pH regulation (Smith & Raven, 1979) are: H^+ binding by cytosolic buffering groups; and H^+ transport out of the cytosol, either across the plasma membrane or across the vacuolar membrane. The transmembrane H^+ fluxes have to be electrically compensated by other ion fluxes (e.g. parallel anion fluxes or opposite cation fluxes). While the fundamental mechanisms of short-term pH regulation are well established, in plant cells we are lacking a comprehensive quantitative model of the processes involved.

Algae and higher plants show considerable variation in their tolerance to acidic environments; some algae can even live at pH 3.0 and lower (Weber *et al.*, 2007). We are only beginning to understand the physiological differences causing this variation in acid tolerance (Messerli *et al.*, 2005). Here, the acidophilic, unicellular green alga *Eremosphaera viridis* was used to develop a comprehensive and quantitative picture for short-term pH regulation. A mathematical model was developed to calculate the following: the permeability of the plasma membrane for weak acid; the cytosolic buffer capacity; the amount of H^+ pumped out of the cell; and the amount of H^+ pumped into the vacuole. In this context the use of weak lipophilic acids to determine cytosolic buffer capacities and the use of butyrate

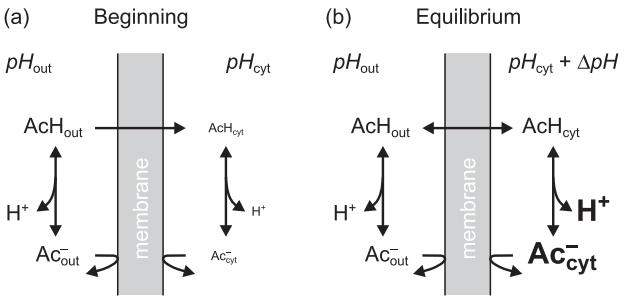

Fig. 1 Cytosolic acidification by weak acids. At the start (a) the protonated, membrane-permeable form of the weak acid, acetic acid (AcH), driven by its concentration gradient, diffuses into the cell. Inside the cell, AcH dissociates into Ac^- and H^+, acidifying the cytosol. Equilibrium (b) is reached when the concentration of AcH outside and inside the cytosol is the same.

to 'clamp' the cytosolic pH are critically discussed. The ion fluxes that accompany – and electrically compensate – regulatory H^+ fluxes were identified. Based on this comprehensive analysis, the ATP demand for short-term pH regulation is calculated. The quantitative analysis presented here provides a solid foundation to investigate the role of cytosolic pH changes in intracellular signaling, allows calculation of the bioenergetic cost of pH regulation, and gives insight into cytosolic pH regulation in an acidophilic alga.

Materials and Methods

Plant material

The coccal green alga *Eremosphaera viridis* de Bary (LB 228-1; Algal Culture Collection, Göttingen, Germany) was cultivated as described previously (Köhler *et al.*, 1983). Experiments were performed in artificial pond water, containing 0.1 mM KNO_3, 0.1 mM $MgCl_2$, 0.2 mM $CaCl_2$ and 2 mM Mes/NaOH pH 5.6 (~0.4 mM Na^+). Respiration rates and photosynthetic O_2 evolution were measured using a Clark-type O_2 electrode (Bachofer, Reutlingen, Germany). Photosynthesis was measured with saturating white light (350 W m^{-2}) at a constant temperature of 20°C. O_2 evolution rates were related to chlorophyll, which was quantified after extraction in 80% acetone (Röbbelen, 1957).

Electrophysiological recordings

Experiments were performed with photosynthetically saturating white light at a temperature of 20 ± 2°C under continuous bath perfusion (200 ml h^{-1}). At a bath volume of 0.2 ml, complete exchange of bath solution (more than three bath volumes) took 10–15 s. For impalements, algae with diameters of at least 150 μm were selected (full-grown cells without indications of cleavage), with a spherical shape and a dark green color. Membrane resistance was measured with two impaled microelectrodes; one electrode was used to inject a current of 0.1 nA for 400 ms every 10 s while the other electrode registered the resulting membrane potential change (membrane resistance = membrane potential change/injected current). Intracellular ion activities were measured using ion-selective liquid membrane microelectrodes (Ammann, 1986), as described in detail earlier (Bethmann *et al.*, 1995, 1998). Sensors for ion-selective microelectrodes were from Fluka (H^+ ionophore no. 95297, K^+ ionophore no. 60398, 10% (w/w) Na^+ ionophore ETH 227 in *o*-nitrophenyloctyl ether). Because ion-selective microelectrodes respond to ion activity as well as to membrane potential, a synchronous measurement of the transmembrane electrical potential has to be performed. This was carried out using a separate voltage electrode or, alternatively, a theta-shaped double-barreled glass-capillary containing both electrodes. See Bethmann *et al.* (1995) for a discussion of the advantages and disadvantages of these two different approaches. Nonturgor-resistant ion-selective microelectrodes were used. Impalement was made possible by turgor reduction, which was achieved by adding 400 mM sorbitol to artificial pond water (Bethmann *et al.*, 1995, 1998). As shown earlier (Thaler *et al.*, 1992), neither the steady-state value nor the light-dependent changes of the membrane potential are altered by sorbitol at this concentration. Also, photosynthetic O_2 evolution and respiratory O_2 consumption are not affected. Moreover, it was shown that turgor decrease by high concentrations of nonelectrolytes does not cause ion uptake in *Eremosphaera* (Frey *et al.*, 1988). Electrode potentials were measured using a high-input impedance amplifier and registered by a pen recorder. Calibration of the ion-selective electrode was performed before and after each measurement. Ion activities are based on the calibration after each recording, because small changes in electrode characteristics can be caused by impalement. The resistance of the ion-selective electrode was routinely checked during the experiment to ensure the integrity of the sensor. Membrane potentials are related to a reference point outside the cytosol (Bertl *et al.*, 1992).

Data analysis and mathematical modeling

Results are stated as mean ± SE with the number of cells given in parentheses. For kinetic analysis, original recordings (chart paper) were scanned and image files were transformed into x-y-data files using a program written by the authors. Nonlinear regression analysis based on the Marquardt algorithm was performed using GRAPHPAD PRISM 5.0 (GraphPad Software, Inc., La Jolla, CA, USA). To model cytosolic pH changes Eqns 5 and 8 were solved numerically USING MATHEMATICA 6 (Wolfram Research, Inc., Champaign, IL, USA).

Results

Cytosolic acidification by weak lipophilic acids

To investigate short-term cytosolic pH regulation in the acidophilic unicellular green alga *E. viridis*, the cytosol was acidified

by adding the lipophilic weak acids acetate or propionate to the perfusion solution (Fig. 1). To estimate the range where cytosolic acidification had a physiological effect, dark respiration was measured at different acetate concentrations. At an external pH of 5.6, the perfusion of 0.1, 1.0 or 10 mM acetate (0.012, 0.12 or 1.2 mM membrane-permeable acetic acid (AcH), respectively) had no significant effect on respiration in *Eremosphaera*. Instead of further increasing the acetate concentration in the perfusion medium, the external pH was lowered to $pH_{out} = 4.6$ to increase the concentration of AcH, the protonated membrane-permeable form. At pH 4.6, the perfusion of 10 mM acetate (5.9 mM AcH) resulted in a doubling of the rate of respiration, from 1.4 to 2.8 mol O_2 (mol Chl h)$^{-1}$ (Supporting Information Fig. S1a). Propionate had an effect on respiration that was comparable to that of acetate. Photosynthetic oxygen evolution at $pH_{out} = 4.6$ was more sensitive against perfusion of acetate. From a slight decrease at 2 mM acetate, oxygen evolution had completely vanished at 10 mM acetate (Fig. S1b). Millimolar concentrations of acetate at $pH_{out} = 4.6$ resulted in a cytosolic acidification that affected both respiration and photosynthesis.

Control measurements showed that a decrease in the external pH from 5.6 to 4.6 did not affect the rate of photosynthesis (70 ± 5 mol O_2 (mol Chl h)$^{-1}$; $n = 14$) or the rate of respiration (approx. −2% of the photosynthesis rate; $n = 16$). Even a decrease of the external pH value to 3.0 had no effect on photosynthetic O_2 evolution. A decrease of the external pH from 5.6 to 4.6 did result in a depolarization, $\Delta E = 11$ mV, and a slight decrease in plasma membrane resistance, but no significant change in cytosolic pH and K^+ concentration (Table S1). A decrease of the external pH from pH 5.6 to pH 3.6 resulted in a more pronounced depolarization ($\Delta E = 19 \pm 2$ mV, $n = 14$) of the plasma membrane and a small, but significant, cytosolic acidification ($\Delta pH_{cyt} = -0.09 \pm 0.01$, $n = 14$). Being adapted to an acidic environment – *Sphagnum* bogs – *Eremosphaera* is obviously little affected by a moderate acidification of the perfusion medium.

Applying a constant dose of acetate over different time intervals

To allow a quantitative analysis of cytosolic pH changes, constant doses of the weak lipophilic acid acetate were applied to single algal cells over different periods of time, as follows: 1 mM acetate ($AcH = 0.59$ mM; $pH_{out} = 4.6$) was perfused for 30 min, 2 mM acetate ($AcH = 1.17$ mM) was perfused for 15 min, 4 mM acetate ($AcH = 2.34$ mM) was perfused for 7.5 min, or 10 mM acetate ($AcH = 5.9$ mM) was perfused for 3 min. By doubling the external concentration of weak acid the driving force for uptake, and thus the influx rate, was doubled. Reducing the perfusion time to 50%, while doubling the influx rate, resulted in the same total amount (constant dose) of weak acid loaded into the cell. Using pH-selective microelectrodes the membrane potential and the cytosolic pH value were recorded during the four different acetate perfusion regimes (Fig. 2). Obviously, cytosolic acidification was not the same for the four different perfusion protocols. At 1 mM acetate, cytosolic acidification was rather small and was back regulated already during the 30-min perfusion interval. The membrane potential either showed a slight hyperpolarization or a depolarization as it was observed at higher acetate concentrations (Fig. 2). Increasing acetate concentrations resulted in increasing rates of acidification, increasing maximum acidifications at the end of acetate perfusion and increasing rates of recovery after acetate perfusion was stopped. Recovery of cytosolic pH was usually complete within 10 to 15 min (Fig. 2, Table 1). Control experiments with 2 and 10 mM propionate instead of acetate showed very similar results with slightly increased cytosolic acidification.

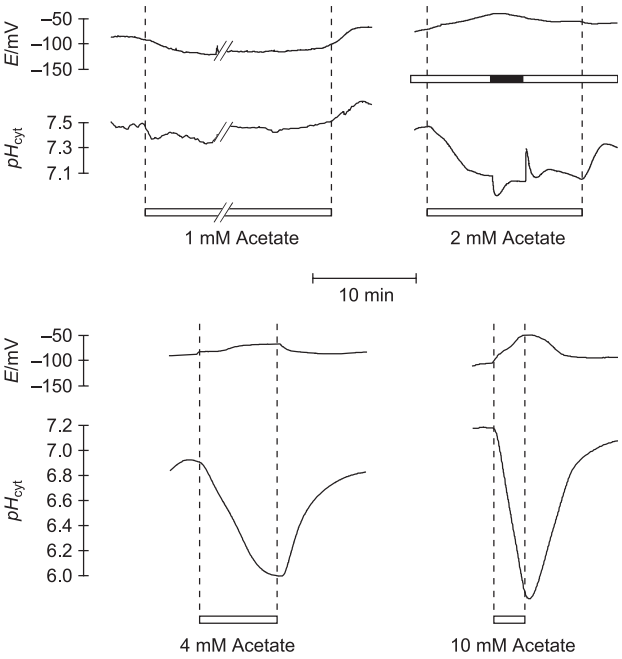

Fig. 2 Effect of acetate on membrane potential, *E*, and cytosolic pH value, pH_{cyt}. Acetate was applied at a constant dose by choosing the perfusion time inversely proportional to the acetate concentration (10 mM for 3 min, 4 mM for 7.5 min, 2 mM for 15 min and 1 mM for 30 min). During the perfusion of 2 mM acetate, the light was switched off for approx 3 min (illumination protocol indicated by black and white bar) to elicit characteristic light-induced cytosolic pH changes. Otherwise all experiments were performed under photosynthetically saturating white light.

To quantify the acidification that is caused by the application of a weak lipophilic acid, one starts with the Henderson–Hasselbalch equation:

$$pH = pK + \log\frac{Ac^-}{AcH} \Leftrightarrow Ac^- = 10^{pH-pK} \cdot AcH, \qquad \text{Eqn 1}$$

where Ac^- and AcH are the concentration of the deprotonated and the protonated form, respectively. With $Ac^- + AcH = Ac_{tot}$, the Henderson–Hasselbalch equation can be rearranged into:

Table 1 Effect of four different acetate concentrations on the cytosolic pH of *Eremosphaera*

[Acetate]	Acidification ΔpH_P	Recovery ΔpH_R	Rate of acidification ΔpH min^{-1}	Rate of recovery ΔpH min^{-1}
1 mM	–0.13 ± 0.04 ($n = 8$)	0.17 ± 0.05 ($n = 4$)	–0.024 ± 0.07 ($n = 8$)	0.048 ± 0.01 ($n = 4$)
2 mM	–0.36 ± 0.06 ($n = 11$)	0.33 ± 0.05 ($n = 7$)	–0.077 ± 0.01 ($n = 11$)	0.15 ± 0.01 ($n = 8$)
4 mM	–0.76 ± 0.05 ($n = 9$)	0.69 ± 0.08 ($n = 7$)	–0.17 ± 0.01 ($n = 9$)	0.22 ± 0.01 ($n = 9$)
10 mM	–1.08 ± 0.02 ($n = 15$)	1.04 ± 0.08 ($n = 8$)	–0.49 ± 0.04 ($n = 15$)	0.36 ± 0.04 ($n = 8$)

Acetate was applied at a constant dose by choosing a perfusion time inversely proportional to the acetate concentration (10 mM for 3 min, 4 mM for 7.5 min, 2 mM for 15 min and 1 mM for 30 min). The maximum ('Peak') acidification, ΔpH_P, was determined as the difference between the start pH and the lowest pH values measured immediately after stopping the perfusion of acetate. The recovery, ΔpH_R, was determined as the difference between the lowest pH values measured immediately after stopping the perfusion of acetate and the first stable pH value measured a few minutes later. Rates were determined from the pH change over the first 2 min after changing the perfusion solution.

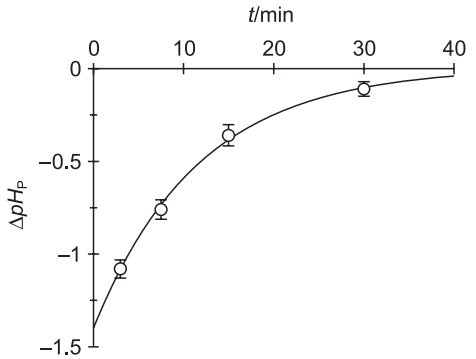

Fig. 3 Maximum cytosolic acidification, ΔpH_P, as a function of perfusion time, *t*. Acetate was applied at a constant dose by choosing a perfusion time inversely proportional to the acetate concentration (10 mM for 3 min, 4 mM for 7.5 min, 2 mM for 15 min and 1 mM for 30 min). The data points were fitted by an exponential function $\Delta pH_P = off + B \cdot \exp(-t/t_0)$ with $off = -0.01$, $B = -1.40$ and $t_0 = 11.7$ min ($R^2 = 0.997$).

$$AcH = \frac{Ac_{tot}}{1+10^{pH-pK}} \text{ or } Ac^- = \frac{Ac_{tot}}{1+10^{pK-pH}}. \qquad \text{Eqn 2}$$

When lipophilic weak acids are applied, it is usually assumed that equilibrium ($AcH_{cyt} = AcH_{out}$; Fig. 1) is rapidly reached. Knowing the cytosolic pH and the concentration of AcH at equilibrium in the cytosol, the concentration of Ac^- in the cytosol, Ac^-_{cyt}, can be calculated (Eqn 1). This concentration corresponds to the amount of H^+ loaded into the cell by the dissociation of AcH. Assuming that during the time of weak acid perfusion pH regulation can be neglected, the buffer capacity is calculated as $\beta = Ac^-_{cyt}/pH$. Values calculated for β in this way (Table S2) range from β = 103 mM at 10 mM acetate (3 min) to β = 1185 mM at 1 mM acetate (30 min). These values are far too high and do depend on the duration of acetate perfusion. Apparently, this simple approach is not suitable for determining reliably the cytosolic buffer capacity. Probably one, or even both (see below), of the initial assumptions – equilibration and no significant pH regulation during the perfusion interval – are wrong.

To analyze further the relation between the perfusion protocol and cytosolic acidification, the amplitude of maximum cytosolic acidification, ΔpH_P, was plotted against perfusion time, *t* (Fig. 3). The shorter the perfusion time – and the higher the external acetate concentration – the higher is ΔpH_P, with an extrapolated maximum of –1.4 pH units at perfusion time $t = 0$. At the other extreme, if low acetate concentrations are perfused over correspondingly long periods of time, there is hardly any cytosolic acidification. This indicates that simple models, on how cytosolic acidification by weak acids works, do not hold. If the assumptions of rapid equilibration of AcH and no significant pH regulation during the acetate perfusion time did hold, one would expect the same acidification for all perfusion times because the total dose of H^+ loaded into the cell is the same for all four perfusion regimes. To describe how cytosolic acidification by weak acids works, and to understand how pH homeostasis in a green plant cell reacts to this acidification, a quantitative model has to be developed.

A mathematical model for cytosolic pH changes caused by weak acids

The total cytosolic concentration of weak acid, Ac_{tot}, results from influx of the acid, AcH, driven by the concentration difference, $AcH_{out} - AcH_{cyt}$ (Fig. 1). The permeability, *P*, of the plasma membrane for the weak acid, the cell-surface area, *A*, and the cytosolic volume, V_{cyt}, determine how rapidly Ac_{tot}, increases. This can be summarized as:

$$\frac{dAc_{tot}}{dt} = (AcH_{out} - AcH_{cyt})\frac{P \cdot A}{V_{cyt}}. \qquad \text{Eqn 3}$$

The cytosolic pH change, dpH_{cyt}/dt, is caused by deprotonation of acetic acid (Fig. 1), and is attenuated by the buffer capacity, β:

$$\frac{dpH_{cyt}}{dt} = -\frac{dH^+_{cyt}}{dt} \cdot \frac{1}{\beta} = -\frac{dAc^-_{cyt}}{dt} \cdot \frac{1}{\beta}. \qquad \text{Eqn 4}$$

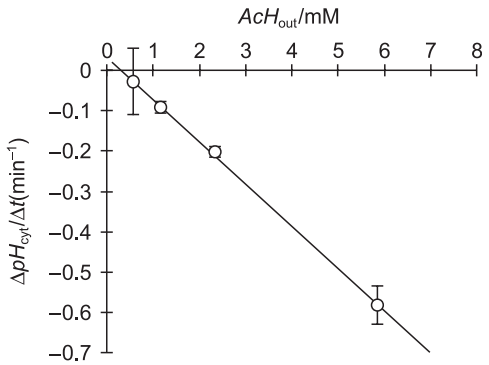

Fig. 4 Initial rate of cytosolic acidification, $\Delta pH_{cyt}/\Delta t$, as a function of the external concentration of acetic acid, AcH_{out}. Values for the acidification rate over the first 2 min (after starting the perfusion of acetate) from Table 1 were multiplied by a factor of 1.185 (according to Fig. 3) to calculate initial acidification rates ($\Delta pH_{cyt}/\Delta t$ at $t = 0$). Data points were described by a linear trend line with a slope of –0.1048 min^{-1} mM^{-1} and an offset of 0.0353 min^{-1}, $R^2 = 0.9994$. The 95% CI for the *y*-axis intercept ranged from 0.0116 to 0.0606 min^{-1}, and an *F* test gave a 2.4% probability for a straight line through the origin (i.e. the *y*-axis intercept is significantly different from zero).

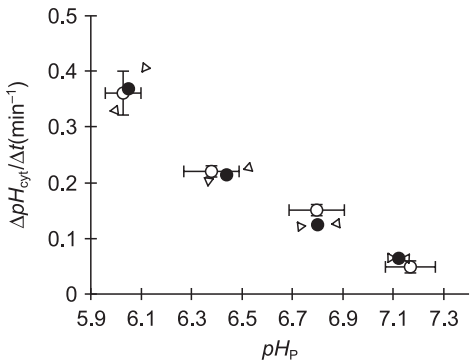

Fig. 5 Initial rate of cytosolic pH recovery ($\Delta pH_{cyt}/\Delta t$ in min^{-1}) as a function of pH at the end of acetate perfusion, pH_P. Data points (open circles; Table 1) resulted from pH recordings (Fig. 2). Calculated points (closed circles) were obtained with Eqns 5 and 8 for $V_{cyt}/A = 6.3$ µm, $P = 3.3\ 10^{-7}$ m s^{-1}, $\beta = 30$ mM, $t_R = 500$ s, $pH_S = pH_{Start} = 7.2$ and $eff = 0.0353$ min^{-1}. Open triangles indicate how calculated points change when β and t_R are changed by 20%.

Deprotonation of acetic acid entering the cytosol via the plasma membrane is instantaneous (< 1 ns). Therefore, acidification is initially restricted to the cytosol, and only once AcH_{cyt} significantly increases does a delayed acidification of cellular organelles occur (described later). The cytosolic buffer capacity, β, was assumed to be constant and not dependent on cytosolic pH, because titration experiments have indicated little pH dependency of β between pH 7.5 and 5.8 (Reid *et al.*, 1989b; Takeshige & Tazawa, 1989).

Substituting AcH_{cyt} in Eqn 3 according to Eqn 2 results in:

$$\frac{dAc_{tot}}{dt} = (AcH_{out} - \frac{Ac_{tot}}{1+10^{pH-pK}})\frac{P \cdot A}{V_{cyt}}. \qquad \text{Eqn 5}$$

Substituting Ac^-_{cyt} in Eqn 4 according to Eqn 2 followed by differentiation and rearranging (see Supporting Information Notes S1) results in:

$$\frac{dpH_{cyt}}{dt} = (\frac{Ac_{tot}}{1+10^{pH-pK}} - AcH_{out}) \cdot \frac{1+10^{pK-pH}}{(\ln(10) \cdot 10^{pK-pH} \cdot Ac_{tot}) + (1+10^{pK-pH})^2 \cdot \beta} \cdot \frac{P \cdot A}{V_{cyt}}. \qquad \text{Eqn 6}$$

Eqns 5 and 6 describe the cytosolic pH change caused by weak acids in the absence of any pH regulation ($\Delta H^+_{cyt} = \Delta Ac^-_{cyt}$). There are only two unknown parameters, namely the buffer capacity of the cytosol, β, and the permeability, *P*, of the plasma membrane for weak acid.

To estimate these two unknown parameters, the initial rates of acidification – when acetate perfusion was started – and the initial rates of re-alkalinization – when acetate perfusion was stopped – were analyzed. The initial rate of acidification contains information about how quickly AcH can enter the cell (i.e. the permeability, *P*) and how well the cytosol is buffered (i.e. the buffer capacity, β). The rates of acidification given in Table 1 were measured over the first 2 min, which is about 10 times more than the time interval for complete exchange of the bath solution. However, Fig. 3 indicates that measuring after 2 min results in an underestimation of the acidification. Therefore, the exponential fit from Fig. 3 was used to correct acidification rates by multiplication with a factor of 1.185 ($\Delta pH_P(t = 0$ min$)/\Delta pH_P(t = 2$ min$) = -1.41/-1.19 = 1.185$). As seen in Fig. 4, the initial rate of acidification is linearly related to the external concentration of acetic acid, AcH_{out}. This is expected from Eqn 6. At the moment when perfusion is started the total acetate concentration in the cytosol, Ac_{tot}, is still zero. For $Ac_{tot} = 0$, Eqn 6 becomes:

$$\frac{dpH_{cyt}}{dt} = \frac{-AcH_{out}}{(1+10^{pK-pH})\beta} \cdot \frac{P \cdot A}{V_{cyt}} \approx \frac{-AcH_{out}}{\beta} \cdot \frac{P \cdot A}{V_{cyt}}. \qquad \text{Eqn 7}$$

With $pK = 4.75$ and $pH = 7.2$ the term $1 + 10^{pK-pH}$ (= 1.0035) comes very close to one, and can thus be disregarded. Plotting the initial rate of acidification, $\Delta pH_{cyt}/\Delta t$, against AcH_{out} in Fig. 4 results in a straight line with a slope of $-P\,A/(\beta V_{cyt})$. With a slope of –0.1048 min^{-1} mM^{-1}, one can calculate $PA/V_{cyt} = 1.747\ 10^{-3}$ s^{-1} mM^{-1} β, or with $V_{cyt}/A = 6.3$ µm, $P = 11\ 10^{-9}$ m s^{-1} mM^{-1} β. This reduces two unknown parameters to one.

The plot of $\Delta pH_{cyt}/\Delta t$ against AcH_{out} is linear – as expected (Fig. 4). However, the regression line does not go through the origin but has a significant, positive offset of +0.0353 min^{-1}. Obviously, a constant offset in the absence of any cytosolic acidification ($AcH_{out} = 0$) does not make sense because it would result in a constant alkalinization of the cytosol. This positive offset can be explained by a pH regulation mechanism, which is activated at small cytosolic acidifications ($AcH_{out} = 0.59$ mM) and removes H^+ from the cytosol at a constant rate (0.0353 min^{-1}).

The initial rate of re-alkalinization – at the moment when acetate perfusion is stopped – contains information about cytosolic pH regulation, at maximum cytosolic acidification. As the question is how cytosolic pH regulation reacts to a certain pH deviation, the initial rate of re-alkalinization, $\Delta pH_{cyt}/\Delta t$, was plotted against the minimum pH, pH_p, at the end of the acetate perfusion period (Fig. 5). This plot shows that the larger the acidification of the cytosol, the larger the rate of pH recovery, indicating a proportional pH regulation mechanism.

To account for the two different cytosolic pH regulation mechanisms indicated by Figs 4 and 5, two terms are added to Eqn 6:

$$\frac{dpH_{cyt}}{dt} = \left(\frac{Ac_{tot}}{1+10^{pH-pK}} - AcH_{out}\right) \cdot \frac{1+10^{pK-pH}}{(\ln(10)\cdot 10^{pK-pH}\cdot Ac_{tot}) + (1+10^{pK-pH})^2 \cdot \beta} \cdot \frac{P\cdot A}{V_{cyt}} + \frac{pH_S - pH(t)}{t_R} + eff. \quad \text{Eqn 8}$$

The term *eff* reflects the pH regulatory mechanism that removes H^+ from the cytosol at a constant rate – according to Fig. 4, *eff* = 0.0353 min^{-1}. The term $(pH_S - pH(t))/t_R$ describes the proportional pH regulation indicated by Fig. 5. Cytosolic pH recovery is proportional to the difference between the actual pH value, $pH(t)$, and a 'set point' value, pH_S. The rate of pH recovery is given by the proportional factor or time constant t_R, with smaller values for higher rates of pH regulation.

The mathematical model given by Eqns 5 and 8 describes the cytosolic pH change caused by a weak lipophilic acid including two simple pH regulatory mechanisms. This model includes three parameters – β, *P* and t_R – that need to be estimated. From Fig. 4, $P = 11\ 10^{-9}$ m s^{-1} mM^{-1} β was calculated, reducing it to two unknown parameters.

Reasonable values for β and t_R were estimated by applying the mathematical model with different sets of values for β and t_R. Eqns 5 and 8 were used to calculate pH_p and Ac_{tot} for the end point of the four different perfusion regimes (Fig. 2) with different values for β and t_R. The resulting pH_p and Ac_{tot} values were used to calculate the corresponding $\Delta pH_{cyt}/\Delta t$ values immediately after acetate perfusion was stopped (Eqn 8 with $AcH_{out} = 0$). This was repeated with different values for β and t_R, and the quadratic deviation between measured and calculated

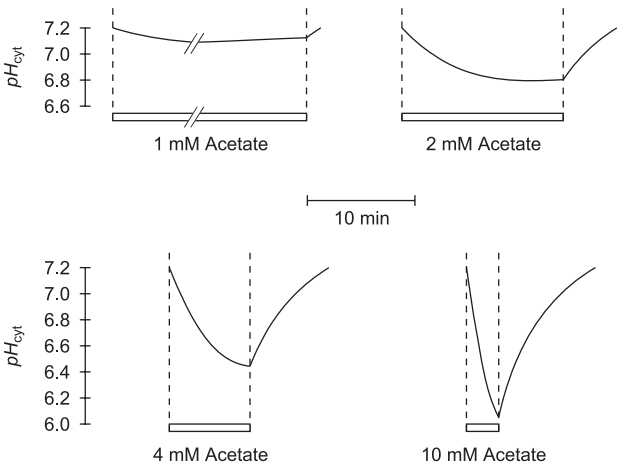

Fig. 6 The time course of cytosolic pH changes upon perfusion of different acetate concentrations was calculated using Eqns 5 and 8 for $V_{cyt}/A = 6.3$ µm, $P = 3.3\ 10^{-7}$ m s^{-1}, β = 30 mM, $t_R = 500$ s, $pH_S = pH_{Start} = 7.2$ and *eff* = 0.0353 min^{-1}.

values (Fig. 5) for pH_p and $\Delta pH_{cyt}/\Delta t$ was calculated. The values for β and t_R were systematically varied to minimize the quadratic deviation. For β = 30 mM and t_R = 500 s the quadratic deviation had a minimum and the set of values calculated (closed circles) for both pH_p and $\Delta pH_{cyt}/\Delta t$ came very close to the experimentally determined values (open circles) at all four acetate concentrations (Fig. 5). With β = 30 mM the relation obtained from Fig. 4, $P = 11\ 10^{-9}$ m s^{-1} mM^{-1} β, resulted in $P = 3.3\ 10^{-7}$ m s^{-1}.

The mathematical model was validated by inserting the complete set of parameters ($A = 0.071$ mm^2, $V_{cyt} = 0.45$ nl, $P = 3.3\ 10^{-7}$ m s^{-1}, β = 30 mM, $t_R = 500$ s, and *eff* = 0.0353 min^{-1}) into Eqns 5 and 8 to calculate the time course of acetate-induced cytosolic pH changes in *Eremosphaera*. These calculated pH traces (Fig. 6) display all the characteristic features of recorded pH traces (Fig. 2). The main difference seems to be a low pass filtering of the recorded pH traces, as a result of the time it takes to exchange the bath solution (10–15 s) and because of the response time of ion-sensitive microelectrodes (2–4 s). The re-alkalinization of the calculated traces approaches pH values of > 7.5, as a result of the pH regulation by constant H^+ removal – represented by *eff*. In Fig. 6 the re-alkalinization phase is cut off as soon as $pH_{cyt} = pH_{Start} = 7.2$ is reached. It can be assumed that the constant H^+ removal stops (*eff* = 0) as soon as a physiological pH or a certain set point in the cytosol is reached. This would explain the biphasic re-alkalinization frequently observed – at the moment the *eff* component is 'switched off' the slope of the re-alkalinization phase is decreased. The mathematical model (Eqns 5 and 8) qualitatively describes the time course of the acetate-induced cytosolic pH changes (Fig. 6) and quantitatively describes the amplitude of those changes as well as the initial acidification and re-alkalinization rates (Fig. 5).

Values for cytosolic acidification, pH_p, the cytosolic concentration of deprotonated acetate, Ac^-_{cyt}, and the cytosolic concentration of acetic acid, AcH_{cyt}, at the end of acetate perfusion

Table 2 Calculated values for the cytosolic acidification, pH_P, the cytosolic concentration of deprotonated acetate, Ac^-_{cyt}, and the cytosolic concentration of acetic acid, AcH_{cyt}

[Acetate]	AcH_{out} (mM)	pH_P	Ac^-_{cyt} (mM)	AcH_{cyt} (mM)	Percentage H^+ buffered	Percentage H^+ proportional regulation	Percentage H^+ constant efflux
1 mM	0.59	7.12	44.89	0.19	5.0	23.4	70.8
2 mM	1.17	6.80	45.23	0.40	26.3	38.0	35.1
4 mM	2.34	6.44	45.17	0.92	50.3	31.0	17.6
10 mM	5.8	6.05	45.80	2.28	75.1	16.7	6.9

Values were calculated, using Eqns 5 and 8, for the end point of the different acetate-perfusion times with $V_{cyt}/A = 6.3$ µm, $P = 3.3\ 10^{-7}$ m s^{-1}, $\beta = 30$ mM, $t_R = 500$ s, $pH_S = pH_{Start} = 7.2$ and $eff = 0.0353$ min^{-1}. The percentage of H^+ buffered were calculated using $(\Delta pH_P\ \beta)/\ Ac^-_{cyt}$ (assuming the total proton load $H^+_{cyt} = Ac^-_{cyt}$), the percentage of H^+ removed by proportional pH regulation were calculated using Eqns 5 and 8, and the percentage of H^+ removed by constant efflux were calculated by multiplying the constant pump rate of 0.0353 min^{-1} with buffer capacity, β, and perfusion time.

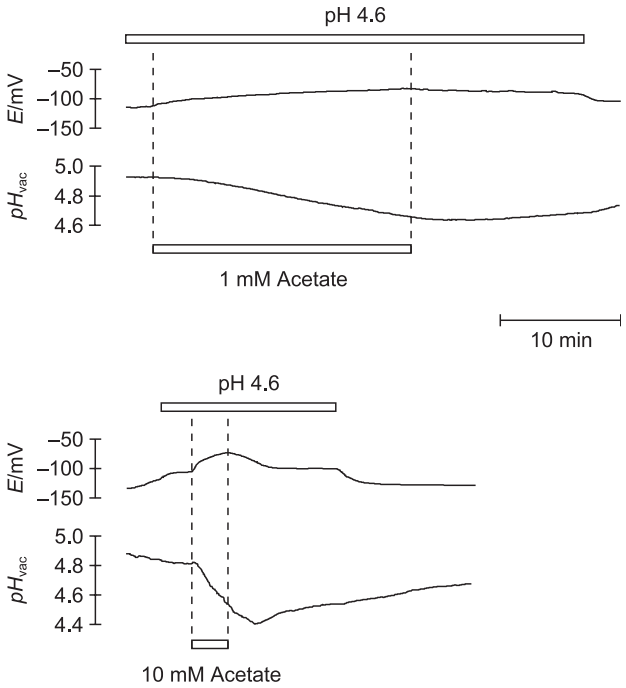

Fig. 7 Effect of acetate on membrane potential, *E*, and on vacuolar pH value, pH_{vac}. Starting from an external pH of 5.6, the external pH was decreased to pH 4.6 and then acetate (1 mM for 20 min, top, or 10 mM for 3 min, bottom) was added.

were calculated (Table 2). The values obtained showed that the original concept of constant acetate doses generally holds – the total concentration of H^+ loaded into the cells ($H^+_{cyt} = Ac^-_{cyt}$) differed by < 1 mM (2%). Even with perfusion times of 30 min (1 mM acetate), equilibrium was not reached (Table 2). For all four perfusion regimes, the cytosolic AcH concentration was less than half of the external concentration. This demonstrates that reaching a stable or maximum cytosolic pH does not imply that equilibrium ($AcH_{cyt} = AcH_{out}$) has been reached. The mathematical model was also used to calculate to what extent different pH-regulatory mechanisms contribute to pH homeostasis during the different perfusion regimes. The higher the acetate concentration (and the shorter the corresponding perfusion time), the higher the proportion of H^+ that are bound by cytosolic buffers and the smaller the proportion of H^+ that are removed from the cytosol by pH-regulatory mechanisms – proportional regulation or constant efflux (Table 2). However, even at 3 min of perfusion with 10 mM acetate, approx. 25% of H^+ are not bound by cytosolic buffers, but are removed by other pH-regulatory mechanisms.

The contribution of the vacuole to pH regulation

To determine what might be the contribution of the vacuole to short-term cytosolic pH regulation, vacuolar pH was measured during acetate perfusion. The acidification of the cytosol caused by acetate was accompanied by vacuolar acidification (Fig. 7). The maximum vacuolar acidification, up to 0.6 pH units, varied little (less than a factor of two) between the four different acetate perfusion regimes. The acidification of the vacuole continued for a few minutes after the perfusion of acetate was stopped (Fig. 7). The rate of pH recovery was generally low, and pH recovery was not complete during the time of the recording. The maximum rate of acidification was linearly related to the acetate concentration applied, being -0.020 ± 0.002 ($n = 4$), -0.041 ($n = 1$), -0.080 ($n = 1$) and -0.16 ± 0.03 min^{-1} ($n = 4$) at 1, 2, 4 and 10 mM acetate, respectively.

Two observations indicated that the recorded vacuolar pH changes are caused by pH regulation and do not simply result from passive distribution of AcH. (1) Acidification of the vacuole began almost immediately after starting acetate perfusion – parallel to the cytosolic acidification, at a time when the cytosolic AcH concentration was still very low. (2) The observed acidification is too large to be explained by passive AcH distribution between cytosol and vacuole (see Notes S2). Yet, a small part of vacuolar acidification is probably caused by passive AcH influx from the cytosol. This raises the question of whether active H^+ uptake into the vacuole is part of the proportional pH regulation (term $(pH_S - pH(t))/t_R$ in Eqn 8) or the constant H^+ efflux

(*eff* in Eqn 8), or both. Constant H^+ efflux into the vacuole would result in the same rate of acidification at all four acetate concentrations, and an increasing maximum acidification with increasing perfusion times. This is clearly not the case for the vacuolar acidification observed here (Fig. 7). The linear increase in the rate of acidification with acetate concentration is expected for a proportional pH-regulatory mechanism (Table 2). It can therefore be concluded that the proportional pH-regulatory mechanism (term $(pH_S - pH(t))/t_R$ in Eqn 8) reflects H^+ pumping from the cytosol into the vacuole. A vacuolar acidification of up to 0.6 pH units (Fig. 7) at a vacuolar buffer capacity of $\beta_{vac} = 10$ mM corresponds to the uptake of 6 mM H^+. At a volume ratio of 1:3 between cytosol and vacuole, 6 mM vacuolar H^+ are equivalent to 18 mM cytosolic H^+. In relation to the concentration of Ac^- (approx. 45 mM) that accumulates in the cytosol (Table 2), this means that up to 40% of the H^+ load of the cytosol are pumped into the vacuole. This corresponds approximately to the maximum contribution estimated for the proportional pH regulation (Table 2).

The contribution of the plasma membrane H^+-ATPase to pH regulation

The correspondence of H^+ pumping into the vacuole with the proportional pH-regulatory mechanism raises the question of which transport process is responsible for the constant efflux component. H^+ pumping out of the cell by the plasma membrane H^+-ATPase could be responsible for this part of pH regulation. However, there is evidence showing that the plasma membrane H^+-ATPase is activated by cytosolic acidification with a maximum ATPase activity of approx. pH 6.6 (Kurkdjian & Guern, 1989; Lanfermeijer & Prins, 1994). This seems at variance with the assumption of a constant (i.e. largely pH independent) H^+ efflux carried by the plasma membrane H^+-ATPase of *Eremosphaera*. Yet, while ATP hydrolysis measurements show pronounced pH dependence, the pH dependence of H^+ pumping is far less pronounced – especially for mesophyll cells (Becker *et al.*, 1993). Moreover, heterologous expression of tobacco (*Nicotiana plumbaginifolia*) plasma membrane H^+-ATPases in yeast (*Saccharomyces cerevisiae*) demonstrated that different isoforms have different pH dependence (Luo *et al.*, 1999), and single point mutations can change pH dependence and H^+-ATPase activity (Morsomme *et al.*, 1996). It therefore seems reasonable to assume that the plasma membrane H^+-ATPase(s) of *Eremosphaera* in adaptation to the acidic environment (*Sphagnum* bogs) may show a high – and largely constant – pump activity already at relatively small cytosolic acidification. The size of the constant efflux, $eff = 0.0353$ min^{-1} (Fig. 4), can be recalculated into a pump current of 766 pA or 1.1 μA cm^{-2} ($\beta = 30$ mM, $V_{cyt} = 0.45$ nl, $A = 0.071$ mm^2). This pump current is comparable in amplitude to maximum plasma membrane H^+-ATPase pump currents measured using *Vicia faba* mesophyll cells of 1.2 ± 0.2 μA cm^{-2} (Lohse & Hedrich, 1992).

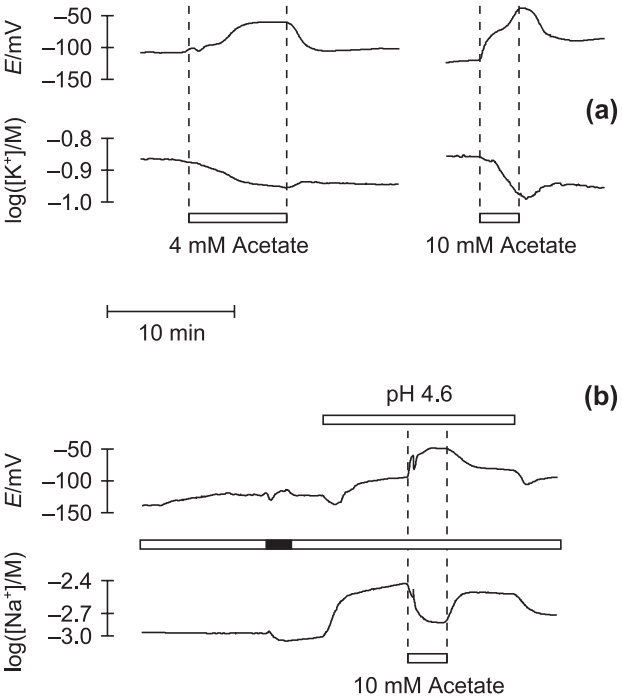

Fig. 8 Effect of acetate on membrane potential, *E*, and on cytosolic K^+ (a) and Na^+ (b) activities. (a) Perfusion of acetate (4 mM for 7.5 min, or 10 mM for 3 min; pH 4.6) resulted in depolarization of the plasma membrane and a decrease in cytosolic K^+ activity. (b) Complete perfusion protocol for a cytosolic Na^+ activity recording. Starting at pH 5.6, transient darkening (black and white bar gives illumination protocol) resulted in a slight decrease of cytosolic Na^+. Changing the pH to 4.6 caused depolarization of the plasma membrane and increase in cytosolic Na^+. Perfusion of 10 mM acetate caused a further depolarization and a reversible decrease of cytosolic Na^+.

Compensating ion fluxes

The mathematical model shows that between 25% (10 mM acetate) and 95% (1 mM acetate; Table 2) of the H^+ loaded into the cytosol are removed by being pumped into the vacuole or out of the cell. Which ion fluxes do electrically compensate these significant H^+ fluxes?

Cytosolic K^+ activity was measured using ion-selective microelectrodes. Perfusion of acetate resulted in a decrease of the cytosolic K^+ activity, $[K^+]_{cyt}$ (Fig. 8a). During acetate perfusion, $[K^+]_{cyt}$ decreased from 183 ± 5 mM to 152 ± 8 mM (4 mM acetate, $n = 7$) or from 187 ± 6 mM to 146 ± 7 mM (10 mM acetate, $n = 9$; the concentrations were calculated from recorded activities with an activity factor of 0.715). After stopping acetate perfusion, within a few minutes the $[K^+]_{cyt}$ had again increased by 10 to 20 mM (Fig. 8a). The decrease in $[K^+]_{cyt}$ recorded during acetate perfusion is probably caused by passive K^+ efflux. Because of a high cytosolic K^+ activity, the electrochemical potential gradient for K^+ favors efflux. An increased conductance of the plasma membrane for K^+ is expected to hyperpolarize

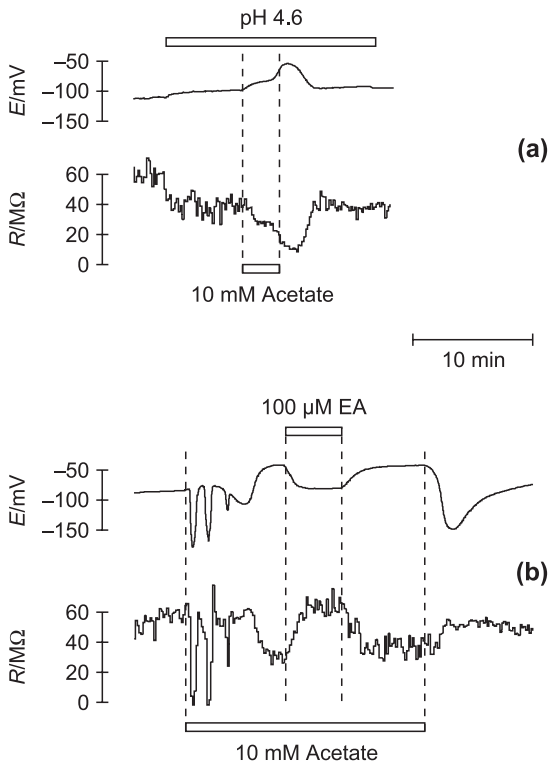

Fig. 9 Effect of acetate on membrane potential, *E*, and membrane resistance, *R*. Small potential spikes resulting from current injection every 10 s were removed from membrane potential recordings. (a) Perfusing 10 mM acetate for 3 min resulted in depolarization of the plasma membrane accompanied by a decrease in membrane resistance. (b) Perfusing 10 mM acetate for 20 min first induced three transient hyperpolarizations before the typical depolarization and decrease in resistance of the plasma membrane was observed. Perfusing 100 mM ethacrynic acid (EA) reversibly repolarized the plasma membrane and increased the membrane resistance.

the membrane, as it is seen in the transient hyperpolarizations in Fig. 9. The observed depolarization of the plasma membrane therefore has to be caused by an increased conductance for other ions. The partial recovery of cytosolic K^+ activity after stopping acetate perfusion is probably caused by K^+ release from the vacuole, which electrically counterbalances electrogenic H^+ pumping into the vacuole. The duration of this increase in $[K^+]_{cyt}$ coincides with the continuing vacuolar acidification after stopping acetate perfusion (Fig. 7). Active uptake of K^+ across the plasma membrane would be accompanied by a parallel uptake of H^+, which should slow down the pH recovery of the cytoplasm. It had been postulated earlier that because of existing ion gradients, electrogenic transport processes across the vacuolar membrane are probably electrically compensated by K^+ fluxes (Bethmann *et al.*, 1995). It seems likely that H^+ transport into the vacuole is electrically compensated by K^+ efflux from the vacuole, and when acetate perfusion was stopped, the ongoing pumping of H^+ into the vacuole (Fig. 7) gave rise to the observed $[K^+]_{cyt}$ recovery (Fig. 8a).

Cytosolic Na^+ activity was measured using ion-selective microelectrodes. Changing the external pH from 5.6 to 4.6 caused an increase of the cytosolic Na^+ activity, $[Na^+]_{cyt}$, by 3–4 mM (Fig. 8b, Table S1). By contrast, perfusion of acetate resulted in a decrease of $[Na^+]_{cyt}$ (Fig. 8b). During perfusion of 10 mM acetate (3 min), $[Na^+]_{cyt}$ decreased from 8.1 ± 1.6 mM ($n = 10$) to 3.2 ± 1.2 mM ($n = 5$). After acetate perfusion was stopped, $[Na^+]_{cyt}$ increased again and partially recovered (Fig. 8b). The increase in $[Na^+]_{cyt}$ recorded at pH 4.6 is probably caused by passive Na^+ influx. As a result of a relatively small concentration gradient ($[Na^+]_{out}$ = 0.4 mM), the electrochemical potential gradient for Na^+ favors influx at physiological membrane potentials. Passive Na^+ influx can electrically compensate H^+ pumping out of the cell. The observed decrease of $[Na^+]_{cyt}$ during acetate perfusion was unexpected and indicates that Na^+ uptake does not contribute to compensate electrogenic H^+ efflux driven by the plasma membrane H^+-ATPase. Instead, Na^+ was removed from the cytosol – parallel to H^+. The partial recovery of $[Na^+]_{cyt}$ after stopping acetate perfusion can be explained by passive Na^+ uptake or by Na^+ release from the central vacuole.

With K^+ and Na^+ not contributing to the electrical compensation of H^+ pumping out of the cell, which ions do electrically compensate H^+ export and what causes the depolarization during acetate perfusion? An increase in the conductivity of the plasma membrane for anions, resulting in anion release from the cytosol, could explain both. As it is not clear which anions might be transported, and because anions are hard to measure directly using ion-selective microelectrodes, a more indirect pharmacological approach was used. The membrane potential and the membrane resistance were measured using two impaled microelectrodes. Changing the external pH from 5.6 to 4.6 caused a slight depolarization and a decrease in membrane resistance (Fig. 9a, Table S1). Perfusion of 10 mM acetate (3 min, Fig. 9a) caused depolarization of the plasma membrane and a parallel decrease of the membrane resistance to 12 ± 1 MΩ ($n = 8$). Obviously, the depolarization of the plasma membrane observed during acetate perfusion (Figs 2, 7–9) was caused by an increase in membrane conductance. To elucidate this membrane conductance further, different inhibitors were applied. A concentration of 10 mM acetate was perfused and when the maximum depolarization was reached an additional inhibitor was perfused (Fig. 9b). Addition of 400 µM $AlCl_3$ ($n = 3$) or 50 µM $ZnCl_2$ ($n = 5$) had no significant effect on membrane potential or resistance. Addition of 100 µM ethacrynic acid ($n = 4$) rapidly hyperpolarized the membrane potential and increased the membrane resistance. This effect of ethacrynic acid was fully reversible (Fig. 9b). When 10 mM acetate and 400 µM ethacrynic acid were perfused together for 6 min, membrane resistance either did not change or slightly increased, and instead of a depolarization a slight hyperpolarization of the plasma membrane was observed. Ethacrynic acid is a well-established inhibitor of plant anion channels (Lunevsky *et al.*, 1983; Schauf & Wilson, 1987; Tyerman, 1992). Probably, the H^+ pumped out of the cell

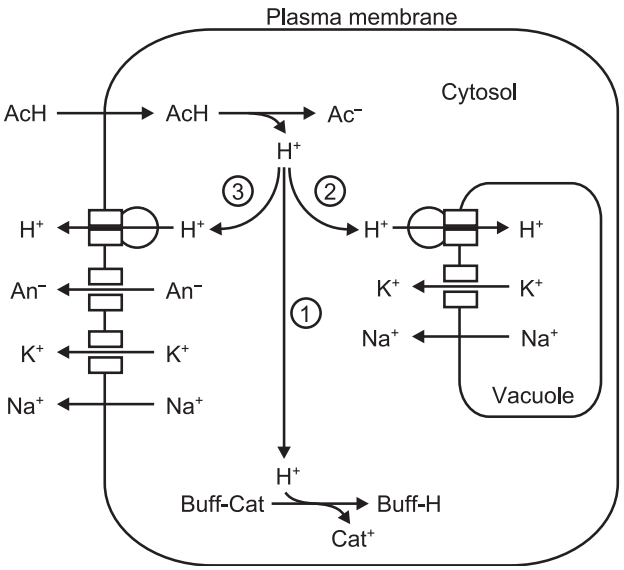

Fig. 10 Scheme of three different pH-regulatory mechanisms in a green plant cell. Influx and deprotonation of acetic acid (AcH) resulted in acidification of the cytosol (top). ① Binding of H^+ to buffer substances attenuates cytosolic acidification. ② Vacuolar proton pumps remove H^+ from the cytosol in a proportional manner – the larger the acidification the higher the pump rate. Uptake of H^+ into the vacuole is electrically compensated by K^+ release. ③ The plasma membrane H^+-ATPase removes H^+ from the cytosol at a constant pump rate – triggered by cytosolic acidification. H^+ efflux out of the cell is electrically compensated by parallel anion efflux. K^+ and Na^+ are released from the cell to adjust osmolarity. H^+ pumps are depicted differently from K^+ and An^- channels to indicate active and passive transport, respectively. AcH is believed to cross the plasma membrane by simple diffusion. The export of Na^+ is either active or, when the membrane is depolarized enough, can be passive.

during acetate perfusion are electrically compensated by parallel passive anion efflux.

Taken together (Fig. 10), our results indicate that H^+ pumping into the vacuole is electrically compensated by K^+ release from the vacuole (Figs 7, 8a), while H^+ pumping out of the cell is electrically compensated by parallel anion efflux (Fig. 9b). This raises the question of why there is such a considerable release of ions during acetate perfusion. Probably K^+, Na^+ and anions are released from the cell to achieve osmotic adjustment. The uptake of about 45 mM AcH (Table 2) during acetate perfusion increases the osmolarity of the cytosol. Perfusion of acetate not only results in acidification of the cytosol but also in a significant increase in osmolarity (Table 2). It seems plausible that the release of K^+ (30–40 mM) and Na^+ (approx. 3 mM), together with anion efflux, compensate for this increase in osmolarity (Fig. 10).

Discussion

Acetate was used as weak lipophilic acid in this study. Control experiments with propionate gave very similar results. Cytosolic acidification of *E. viridis* recorded using 2′,7′-bis-(2-carboxyethyl)-5-(and-6)-carboxyfluorescein (BCECF)–dextran in the presence of different butyrate concentration (Plieth *et al.*, 1997) showed the same amplitudes and kinetics as recorded in this study with acetate (Fig. 2). This indicates that the effects of acetate described here are caused by cytosolic acidification, while the effects on metabolism are negligible. This is in good agreement with earlier results on the effect of different weak lipophilic acids (Frachisse *et al.*, 1988).

The cytosolic buffer capacity, β, of plant cells

The cytosolic buffer capacity (i.e. the amount of H^+ binding by cytosolic buffering groups) was determined in this study to $\beta = 30$ mM for *Eremosphaera*. This corresponds to values determined by titration (Pfanz & Heber, 1986; Reid *et al.*, 1989b; Takeshige & Tazawa, 1989) or gas-exchange and fluorescence methods (Oja *et al.*, 1999) for a variety of green plant cells. By contrast, the published values for β determined using weak acids range from 50 to 160 mM (Frachisse *et al.*, 1988; Grabov & Blatt, 1997; Plieth *et al.*, 1997). As described in the Results, when analyzing experiments that have used weak acids (Eqn 1), it is usually assumed that AcH rapidly equilibrates ($AcH_{cyt} = AcH_{out}$; Fig. 1), and pH regulation is usually not taken into account. Our analysis demonstrates that this approach is too simple (Table S2). Even at perfusion times as short as 3 min, there is considerable pH regulation (25%, Table 2). Even after perfusion times as long as 30 min there is no equilibrium reached between external and cytosolic *AcH* (Table 2). Recording a stable cytosolic pH (Fig. 2) does not mean equilibrium between external and cytosolic concentrations of weak acid, but equilibrium between acidification by AcH influx and pH regulation. In *Eremosphaera*, with a low permeability for acetic acid and a relatively small surface to volume ratio, reaching equilibrium between external and internal *AcH* is expected to take especially long. Yet, measurements on *Acer pseudoplatanus* suspension cells (Guern *et al.*, 1986) showed the same phenomenon. When incubated with 50 mM propionate (pH 6.5) maximum acidification was observed after 1.5 min when < 50% of the equilibrium concentration of radioactive propionate had been taken up. From these data, $\beta = 30$ mM was calculated (Guern *et al.*, 1986), in perfect agreement with the data presented here. Assuming equilibrium ($AcH_{cyt} = AcH_{out}$) has been reached, while it has not, results in an overestimation of cytosolic buffer capacity. This is probably one reason why buffer capacities calculated from perfusion with weak acids are usually overestimated. The other reason is neglecting ongoing pH regulation. Some authors mention that buffer capacities calculated from experiments carried out using weak acids contain a 'dynamic' component (Grabov & Blatt, 1997; Plieth *et al.*, 1997). Yet, we think that it is preferable to separate H^+ buffering by passive ion exchange (i.e. β s.s.) from pH regulation caused by active H^+ transport. The mathematical model introduced here allows this separation. A value of $\beta = 30$ mM reflects the cytosolic buffer capacity of most plant cells.

The permeability, $P = 3.3\ 10^{-7}$ m s^{-1}, of the plasma membrane for acetic acid (AcH) estimated here is at the lower end of published values. The permeability of the plasma membrane for radioactive acetic acid was estimated to $P = 9.6\ 10^{-7}$ m s^{-1} for *Chara corallina* (Reid *et al.*, 1989a), to $P = 30\ 10^{-7}$ m s^{-1} for *Dunaliella parva* (Gimmler & Hartung, 1988) and to $P = 9.1\ 10^{-7}$ m s^{-1} for *Spinacea oleracea* (Gimmler *et al.*, 1981). The relatively low permeability calculated for *Eremosphaera* might reflect an adaptation to the rather acidic environment in which this green alga is living.

Proton pumps involved in pH regulation

Our analysis indicates that both vacuolar H^+ pumps and plasma membrane H^+ pumps are involved in short-term pH regulation. The importance of vacuolar H^+ uptake for short-term cytosolic pH regulation has been established for different plant species (Heber *et al.*, 1994; Romani *et al.*, 1996; Frohnmeyer *et al.*, 1998). When discussing the role of plasma membrane H^+-ATPases in short-term cytosolic pH regulation, one has to keep in mind that *Eremosphaera* is a unicellular alga. For a unicellular organism in an aquatic environment H^+ extrusion by the plasma membrane H^+-ATPase is a 'reasonable option'. By contrast, in a multicellular plant tissue, H^+ excretion into the apoplast might not be a 'reasonable option' because the buffer capacity of the apoplast is usually low (Oja *et al.*, 1999; Felle & Hanstein, 2002) and H^+ excretion could cause deleterious acidification. In single algal cells (Reid *et al.*, 1989b), in suspension cells (Mathieu *et al.*, 1986), in isolated protoplasts (Trofimova, 1992), or in aquatic plants without a defined apoplast (Beffagna & Romani, 1991), plasma membrane H^+-ATPases have been shown to play an important role in short-term cytosolic pH regulation, while in plant tissues of land plants with a defined apoplast the plasma membrane H^+-ATPase seems to play a minor role in short-term pH regulation (Oja *et al.*, 1999; Felle, 2001). The observation that slight cytosolic acidification significantly activates plasma membrane H^+-ATPase proton pumping can probably be explained as an adaptation of *Eremosphaera* to its acidic environment.

Compensating ion fluxes during pH regulation

H^+ transport into the vacuole is probably electrically compensated by cation (K^+ and Na^+) release, while H^+ transport out of the cell is likely to be electrically balanced by parallel anion efflux (Fig. 10). Membrane depolariziation has been observed in *Chara corallina*, upon cytosolic acidification by weak acids (Reid *et al.*, 1989b), which is caused by pH-dependent Cl^- efflux (Johannes *et al.*, 1998). In roots hairs of *Sinapis alba* (Felle, 1987), and for rhizoid cells of the liverwort *Riccia fluitans* (Frachisse *et al.*, 1988), low concentrations of lipophilic weak acids cause a hyperpolarization of the plasma membrane followed by a slow depolarization, while higher concentrations cause an immediate depolarization, as seen here (Fig. 2). At low concentrations of weak lipophilic acid, uptake of monovalent cations was observed. This was interpreted as K^+/H^+ or Na^+/H^+ exchange (Marre *et al.*, 1983; Mathieu *et al.*, 1986), which would allow electroneutral H^+ extrusion from the cell. There is no evidence for K^+ or Na^+ uptake during pH regulation in *Eremosphaera*, and the existing electrochemical driving forces rule out Na^+-driven H^+ extrusion ($\Delta\mu_H = -250$ mV, $\Delta\mu_{Na} = -20$ mV) and make K^+-driven H^+ extrusion ($\Delta\mu_K = +80$ mV) rather unlikely.

In addition to the ion fluxes that electrically counterbalance H^+ pumping, there are indications for a pronounced salt release (approx. 3 mM Na^+ and 30–40 mM K^+) during pH regulation in the presence of weak lipophilic acids. The reason for this salt release is probably osmotic adjustment to compensate for the considerable amount of acetate taken up (approx. 45 mM under the experimental conditions described here) (Table 2). Moreover, the binding of H^+ by cytosolic buffers results in the release of cations – via cation exchange – from those buffers, which can also increase the osmolarity of the cytosol. The transient membrane hyperpolarizations that were sometimes observed when 10 mM acetate was perfused (a small one in Fig. 8b, and two large ones in Fig. 9b) are probably caused by an increase in the cytosolic Ca^{2+} activity as a result of cation exchange (Plieth *et al.*, 1997). It is well established that an increase in cytosolic Ca^{2+} in *Eremosphaera* results in the opening of plasma membrane K^+ channels, giving rise to the observed transient hyperpolarization (Bauer *et al.*, 1998a,b; Schönknecht & Bethmann, 1998) and decrease in membrane resistance, R (Fig. 9b). Incubating plant cells with millimolar concentrations of weak acids not only affects cytosolic pH but also causes considerable increase in osmolarity. In this context, the observation that millimolar concentrations of butyrate prevent or reduce abscisic acid (ABA)-induced stomatal closure might indicate that cytosolic alkalinization, which is prevented by the butyrate 'pH clamp', is an essential signaling step (Blatt & Armstrong, 1993; Wang *et al.*, 2001; Li *et al.*, 2006). Yet, the increase in osmolarity caused by the uptake of significant amounts of butyrate seems likely also to affect stomatal closure.

Energy demand of pH regulation

With the mathematical model it becomes possible to compare the ATP production, as measured via respiration rates, to the theoretical ATP consumption required for the calculated H^+ pumping. Dark respiration rates doubled from 1.4 to 2.8 mol O_2 (mol Chl h)$^{-1}$ under perfusion of 10 mM acetate (at pH 4.6). With 13 mM chlorophyll (in relation to volume of cytoplasm), and assuming an output of 5 ATP/O_2 during respiration, the calculated ATP synthesis rate doubles from 1.5 to 3.0 mM ATP min^{-1} (in relation to the volume of cytoplasm, 0.45 nl) under 10 mM acetate. Compared with this, the constant H^+ efflux, $eff = 0.0353$ min^{-1}, at $\beta = 30$ mM yields a pump rate of 1.06 mM H^+ min^{-1}. With a stoichiometry of 1 ATP/H^+ for the plasma membrane H^+-ATPase (Briskin &

Hanson, 1992) this means that approx. 1 mM ATP min^{-1} is hydrolyzed to drive the constant H^+ efflux out of the cell. The average pump rate for the proportional pH regulation is calculated as 0.35, 1.14, 1.87 and 2.55 mM H^+ min^{-1} for 1, 2, 4 and 10 mM acetate, respectively. With a stoichiometry of 3.4 ATP/H^+ for the vacuolar H^+-ATPase (calculated from Fig. 4 of Kettner *et al.* (2003) with $pH_{cyt} - pH_{vac} = 2.2$), between 0.10 and 0.75 mM ATP min^{-1} (at 1 and 10 mM acetate, respectively) are hydrolyzed to energize the proportional pH regulation by vacuolar H^+ uptake. These calculations show that ATP production by respiration does increase, from 1.5 to 3.0 mM ATP min^{-1}, to cope with the significant ATP demand for H^+ pumping, of up to 1.75 mM ATP min^{-1} at 10 mM acetate.

Acknowledgements

This work was supported by the Deutsche Forschungsgemeinschaft and the National Science Foundation (MCB-0212663). We would like to thank Drs Werner Kaiser, Robert Roelfsema (Würzburg, Germany), Andreas Weber and Andrea Bräutigam (Düsseldorf, Germany) for helpful discussions and suggestions.

References

Ammann D. 1986. *Ion-selective microelectrodes. Principles, design and application*. Heidelberg: Springer-Verlag.

Bauer CS, Plieth C, Bethmann B, Popescu O, Hansen U-P, Simonis W, Schönknecht G. 1998a. Strontium-induced repetitive calcium spikes in a unicellular green alga. *Plant Physiology* **117**: 545–557.

Bauer CS, Plieth C, Hansen U-P, Simonis W, Schönknecht G. 1998b. A steep Ca^{2+}-dependence of a K^+ channel in a unicellular green alga. *Journal of Experimental Botany* **49**: 1761–1765.

Becker D, Zeilinger C, Lohse G, Depta H, Hedrich R. 1993. Identification and biochemical characterization of the plasma-membrane H^+-ATPase in guard cells of *Vicia faba* L. *Planta* **190**: 44–50.

Beffagna N, Romani G. 1991. Modulation of the plasmalemma proton pump activity by intracellular pH in *Elodea densa* leaves – correlation between acid load and H^+ pumping activity. *Plant Physiology and Biochemistry* **29**: 471–480.

Bertl A, Blumwald E, Coronado R, Eisenberg R, Findlay GP, Gradmann D, Hille B, Köhler K, Kolb HA, MacRobbie EAC *et al.* 1992. Electrical measurements on endomembranes. *Science* **258**: 873–874.

Bethmann B, Simonis W, Schönknecht G. 1998. Light-induced changes of cytosolic pH in *Eremosphaera viridis*: recordings and kinetic analysis. *Journal of Experimental Botany* **49**: 1129–1137.

Bethmann B, Thaler M, Simonis W, Schönknecht G. 1995. Electrochemical potential gradients of H^+, K^+, Ca^{2+}, and Cl^- across the tonoplast of the green alga *Eremosphaera viridis*. *Plant Physiology* **109**: 1317–1326.

Blatt MR, Armstrong F. 1993. K^+ channels of stomatal guard cells: abscisic-acid-evoked control of the outward rectifier mediated by cytoplasmic pH. *Planta* **191**: 330–341.

Briskin DP, Hanson JB. 1992. How does the plant plasma membrane H^+-ATPase pump protons? *Journal of Experimental Botany* **43**: 269–289.

Felle H. 1987. Proton transport and pH control in *Sinapis alba* root hairs: a study carried out with double-barrelled pH micro-electrodes. *Journal of Experimental Botany* **38**: 340–354.

Felle HH. 2001. pH: Signal and Messenger in Plant Cells. *Plant Biology* **3**: 577–591.

Felle HH, Hanstein S. 2002. The apoplastic pH of the substomatal cavity of *Vicia faba* leaves and its regulation responding to different stress factors. *Journal of Experimental Botany* **53**: 73–82.

Frachisse J-M, Johannes E, Felle H. 1988. The use of weak acids as physiological tools: a study of the effect of fatty acids on intracellular pH and electrical plasmalemma properties of *Riccia fluitans* rhizoid cells. *Biochimica et Biophysica Acta* **938**: 199–210.

Frey N, Büchner K-H, Zimmermann U. 1988. Water transport parameters and regulatory processes in *Eremosphaera viridis*. *Journal of Membrane Biology* **101**: 151–163.

Frohnmeyer H, Grabov A, Blatt MR. 1998. A role for the vacuole in auxin-mediated control of cytosolic pH by *Vicia* mesophyll and guard cells. *Plant Journal* **13**: 109–116.

Gimmler H, Hartung W. 1988. Low permeability of the plasma membrane of *Dunaliella parva* for solutes. *Journal of Plant Physiology* **133**: 165–172.

Gimmler H, Heilmann B, Demmig B, Hartung W. 1981. The permeability coefficients of the plasmalemma and the chloroplast envelope of spinach mesophyll cells. *Zeitschrift für Naturforschung* **36**: 672–678.

Grabov A, Blatt MR. 1997. Parallel control of the inward-rectifier K^+ channel by cytosolic free Ca^{2+} and pH in *Vicia* guard cells. *Planta* **201**: 84–95.

Guern J, Felle H, Mathieu Y, Kurkdjian A. 1991. Regulation of intracellular pH in plant cells. *International Review of Cytology* **127**: 111–173.

Guern J, Mathieu Y, Pean M, Pasquier C, Beloeil JC, Lallemand JY. 1986. Cytoplasmic pH regulation in *Acer pseudoplatanus* cells: I. A ^{31}P NMR description of acid-load effects. *Plant Physiology* **82**: 840–845.

Heber U, Wagner U, Kaiser W, Neimanis S, Bailey K, Walker D. 1994. Fast cytoplasmic pH regulation in acid-stressed leaves. *Plant and Cell Physiology* **35**: 479–488.

Johannes E, Crofts A, Sanders D. 1998. Control of Cl^- efflux in *Chara corallina* by cytosolic pH, free Ca^{2+}, and phosphorylation indicates a role of plasma membrane anion channels in cytosolic pH regulation. *Plant Physiology* **118**: 173–181.

Kettner C, Bertl A, Obermeyer G, Slayman C, Bihler H. 2003. Electrophysiological analysis of the yeast V-type proton pump: variable coupling ratio and proton shunt. *Biophysical Journal* **85**: 3730–3738.

Köhler K, Geisweid H-J, Simonis W, Urbach W. 1983. Changes in membrane potential and resistance caused by transient increase of potassium conductance in the unicellular alga *Eremosphaera viridis*. *Planta* **159**: 165–171.

Kurkdjian A, Guern J. 1989. Intracellular pH: measurement and importance in cell activity. *Annual Review of Plant Physiology and Plant Molecular Biology* **40**: 271–303.

Lanfermeijer FC, Prins HBA. 1994. Modulation of H^+-ATPase activity by fusicoccin in plasma membrane vesicles from oat (*Avena sativa* L.) roots. A comparison of modulation by fusicoccin, trypsin, and lysophosphatidylcholine). *Plant Physiology* **104**: 1277–1285.

Li S, Assmann SM, Albert R. 2006. Predicting essential components of signal transduction networks: a dynamic model of guard cell abscisic acid signaling. *PLoS Biology* **4**: e312.

Lohse G, Hedrich R. 1992. Characterization of the plasma membrane proton ATPase from *Vicia faba* guard cells. Modulation by extracellular factors and seasonal changes. *Planta* **188**: 206–214.

Lunevsky VZ, Zherelova OM, Vostrikov IY, Berestovsky GN. 1983. Excitation of *Characeae* cell membranes as a result of activation of calcium and chloride channels. *Journal of Membrane Biology* **72**: 43–58.

Luo H, Morsomme P, Boutry M. 1999. The two major types of plant plasma membrane H^+-ATPases show different enzymatic properties and confer differential pH sensitivity of yeast growth. *Plant Physiology* **119**: 627–634.

Marre MT, Romani G, Marre E. 1983. Transmembrane hyperpolarization and increase of K^+ uptake in maize roots treated with permeant weak acids. *Plant, Cell & Environment* **6**: 617–623.

Mathieu Y, Guern J, Pean M, Pasquier C, Beloeil JC, Lallemand JY. 1986. Cytoplasmic pH regulation in *Acer pseudoplatanus* cells: II. Possible mechanisms involved in pH regulation during acid-load. *Plant Physiology* **82**: 846–852.

McLaughlin SG, Dilger JP. 1980. Transport of protons across membranes by weak acids. *Physiological Reviews* **60**: 825–863.

Messerli MA, maral-Zettler LA, Zettler E, Jung SK, Smith PJS, Sogin ML. 2005. Life at acidic pH imposes an increased energetic cost for a eukaryotic acidophile. *Journal of Experimental Biology* **208**: 2569–2579.

Morsomme P, Dexaerde AD, Demeester S, Thines D, Goffeau A, Boutry M. 1996. Single point mutations in various domains of a plant plasma membrane H^+-ATPase expressed in *Saccharomyces cerevisiae* increase H^+-pumping and permit yeast growth at low pH. *The EMBO Journal* **15**: 5513–5526.

Oja V, Savchenko G, Jakob B, Heber U. 1999. pH and buffer capacities of apoplastic and cytoplasmic cell compartments in leaves. *Planta* **209**: 239–249.

Pfanz H, Heber U. 1986. Buffer capacities of leaves, leaf cells, and leaf cell organelles in relation to fluxes of potentially acidic gases. *Plant Physiology* **81**: 597–602.

Plieth C, Sattelmacher B, Hansen U-P. 1997. Cytoplasmic Ca^{2+}-H^+-exchange buffers in green algae. *Protoplasma* **198**: 107–124.

Reid RJ, Smith FA, Soden A, Turnbull AR. 1989a. Regulation of metabolism by intracellular pH: Inhibition of photosynthesis by weak acids in intact cells of *Chara corallina*. *Plant Science* **65**: 15–23.

Reid RJ, Smith FA, Whittington J. 1989b. Control of intracellular pH in *Chara corallina* during uptake of weak acid. *Journal of Experimental Botany* **40**: 883–891.

Röbbelen G. 1957. Bestimmung des Pigmentgehaltes. *Zeitschrift für induktive Abstammungs- und Vererbungslehre* **88**: 189.

Romani G, Beffagna N, Meraviglia G. 1996. Role for the vacuolar H^+-ATPase in regulating the cytoplasmic pH: an *in vivo* study carried out in *chl1*, an *Arabidopsis thaliana* mutant impaired in NO_3^- transport. *Plant and Cell Physiology* **37**: 285–291.

Schauf CL, Wilson KJ. 1987. Properties of single K^+ and Cl^- channels in *Asclepias tuberosa* protoplasts. *Plant Physiology* **85**: 413–418.

Schönknecht G, Bethmann B. 1998. Cytosolic Ca^{2+} and H^+ buffers in green algae: a comment. *Protoplasma* **203**: 206–209.

Smith FA, Raven JA. 1979. Intracellular pH and its regulation. *Annual Review of Plant Physiology* **30**: 289–311.

Takeshige K, Tazawa M. 1989. Measurement of the cytoplasmic and vacuolar buffer capacities in *Chara corallina*. *Plant Physiology* **89**: 1049–1052.

Thaler M, Simonis W, Schönknecht G. 1992. Light-dependent changes of the cytoplasmic H^+ and Cl^- activity in the green alga *Eremosphaera viridis*. *Plant Physiology* **99**: 103–110.

Trofimova MS. 1992. Plasmalemma H^+-ATPase as component of cytosolic pH-stat in isolated protoplasts. *Soviet Plant Physiology* **39**: 1–6.

Tyerman SD. 1992. Anion channels in plants. *Annual Review of Plant Physiology and Plant Molecular Biology* **43**: 351–373.

Wang XQ, Ullah H, Jones AM, Assmann SM. 2001. G protein regulation of ion channels and abscisic acid signaling in *Arabidopsis* guard cells. *Science* **292**: 2070–2072.

Weber APM, Horst RJ, Barbier GG, Oesterhelt C. 2007. Metabolism and metabolomics of eukaryotes living under extreme conditions. *International Review of Cytology – A Survey of Cell Biology* **256**: 1–34.

Supporting Information

Additional supporting information may be found in the online version of this article.

Fig. S1 Dark respiration (a) and photosynthetic oxygen evolution (b) in the presence of different concentrations ofacetate

Notes S1 Derivation of Equation 6

Notes S2 Quantitative estimation of vacuolar acidification

Table S1 Effect of the external pH value on membrane potential, membrane resistance, cytosolic pH, cytosolic potassium activity, and cytosolic sodium activity

Table S2 Hypothetical cytosolic acetate concentrations and buffer capacities

Please note: Wiley-Blackwell are not responsible for the content or functionality of any supporting information supplied by the authors. Any queries (other than missing material) should be directed to the *New Phytologist* Central Office.